INVESTIGATION OF SUBCLINICAL HEMOLYSIS IN AORTIC VALVE STENOSIS USING 4D FLOW MRI-BASED CFD SIMULATIONS

Tianai Wang[1], Christine Quast[2], Florian Bönner[2], Malte Kelm[2,3], Ulrich Steinseifer[1], Michael Neidlin[1]

(1) Department of Cardiovascular Engineering, Institute of Applied Medical Engineering, Medical Faculty, RWTH Aachen University, Aachen, Germany, (2) Department of Cardiology, Pulmonary Diseases and Vascular Medicine, Heinrich-Heine University, Düsseldorf, Germany, (3) CARID, Cardiovascular Research Institute Düsseldorf, Heinrich-Heine University, Düsseldorf, Germany

Introduction

Subclinical hemolysis, release of hemoglobin without the destruction of the red blood cell (RBC) membrane, has been observed in patients with aortic stenosis (AS). Elevated cell-free hemoglobin levels impair nitric oxide bioavailability and promote endothelial dysfunction. Pathological post-valvular blood flow patterns are supposed to induce RBC damage. However, the location of the highest fluid stresses still remains unclear. In this study, we aimed to elucidate the origin of subclinical hemolysis based on in vivo flow measurements through 4D Magnetic Resonance Imaging (4D Flow MRI) and Computational Fluid Dynamics (CFD).

Methods

A computational model of an AS patient aortic geometry was created using medical imaging data. Temporally and spatially resolved boundary conditions taken from 4D Flow MRI measurements were implemented, see left side of Figure 1. A Non-Newtonian fluid model and two turbulent flow models (Reynolds-averaged k-ω SST and scale resolving SBES) were compared. A quantitative comparison between 4D Flow MRI and CFD was performed. Then, the CFD model was used to determine the location and time of highest flow-induced stresses and the role of turbulent flow characteristics.

Results

The overall feasibility of the 4D Flow MRI-based CFD simulation was proven with good agreement between the two velocity data sets and an R^2 of 0.79 ($p<0.001$) in a transversal plane of the ascending aorta, see Figure 1 right. Detailed Bland-Altman analysis revealed that the CFD results systematically underestimate the flow velocities when compared to MRI measurements with a bias of approximately 60 mm/s.

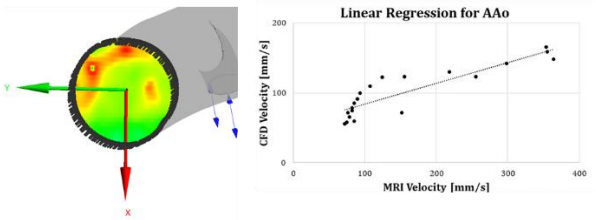

Figure 1: Left: Spatially resolved velocity field from 4D Flow MRI measurements implemented as a boundary condition for CFD. Right: Linear correlation between MRI and CFD velocities in the ascending aorta (AAo).

The left side of Figure 2 shows the resulting shear stress distribution acquired by CFD for a cross-sectional plane in the aorta ascendens during blood flow deceleration after the systolic peak. The turbulence eddy dissipation within the entire aortic arch is shown on the right side of Figure 2.

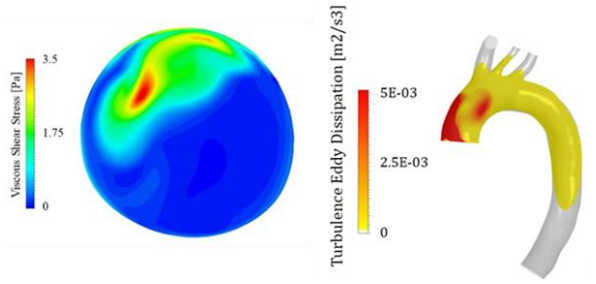

Figure 2: Left: Viscous shear stress distribution on a cross-sectional plane in the aorta ascendens during the deceleration phase of the heart cycle. Right: Corresponding Turbulence Eddy Dissipation in the entire aortic arch.

Viscous shear stresses in the bulk region of the flow with the highest turbulence in the ascending aorta may be the largest contributors to RBC damage. They exceed stresses in the wall region by a factor of four and occur during the flow deceleration phase after the systolic peak. The scale resolving model predicts lower turbulence production than the Reynolds-averaged model. However, the relative contributions of near-wall and free stream stresses remain similar.

Discussion

In summary, a methodology to generate a 4D Flow MRI-based numerical fluid simulation model of AS flow within the aortic arch was developed and validated. Turbulent flow features within the free stream of the ascending aortic jet have been identified as the most prominent contributors towards RBC damage and the onset of subclinical hemolysis.
Future work will validate the results in a higher number of patients and the load on the aortic valve caused by the deteriorated flow structures.

Acknowledgements

This study was funded by the Deutsche Forschungsgemeinschaft (DFG, German Research Foundation) TRR259.